INTERNATIONAL JOURNAL FOR NUMERICAL METHODS IN FLUIDS, VOL. 11, 501–513 (1990)

A FRACTIONAL-STEP TAYLOR–GALERKIN METHOD FOR UNSTEADY INCOMPRESSIBLE FLOWS

H. LAVAL

Commission of the European Communities, Joint Research Centre, Ispra Establishment, I-21020 Ispra (Va), Italy

AND

L. QUARTAPELLE

Istituto di Fisica, Politecnico di Milano, Piazza Leonardo da Vinci 32, I-20133 Milano, Italy

SUMMARY

This paper describes the application of the Taylor–Galerkin method to the calculation of incompressible viscous flows. A finite element fractional-step method for the Navier–Stokes equations is combined with the Taylor–Galerkin method to achieve an accurate treatment of the convection part of the problem. A scheme of second-order accuracy in time for the non-linear convection written in non-conservative form is presented. Numerical results are provided to illustrate the quality of the computed transient solutions in two dimensions.

KEY WORDS Navier–Stokes equations Time-dependent advection-dominated flows Taylor–Galerkin method Finite elements

1. INTRODUCTION

The Taylor–Galerkin method was originally introduced in 1983 to achieve higher-order temporal accuracy in the finite element solution of evolutionary problems describing pure convection.[1,2] The method has been subsequently used to calculate finite element solutions to various kinds of inviscid compressible flows (see Donea *et al.*[3] and the reference therein). Applications to viscous problems have been limited so far to the development of numerical schemes for solving the scalar convection–diffusion equation[4] and for modelling unsteady internal flows in a turbine cascade using the vorticity–streamfunction equations.[5] In both cases the Taylor–Galerkin method has been combined with time-splitting techniques. The aim of the present paper is to describe a Taylor–Galerkin scheme of fractional-step type for the transient solution of the incompressible Navier–Stokes equations expressed in the primitive variables velocity and pressure. Distinct features of the proposed method are a second-order temporal accuracy in highly convective flows and an easy generalization to three-dimensional problems.

The general philosophy behind the proposed approach is that an algorithm is successful whenever its elemental components are designed to deal each with a specific part of the governing equations. To this end, the Navier–Stokes equations are split in time according to the fractional-step method in order to isolate the various spatial differential operators. The temporal approximation of the dynamical effect associated with each operator is then performed through a Taylor expansion to derive the most appropriate time-stepping method. The combination of the Taylor

0271–2091/90/130501–13$06.50

Received April 1989
Revised July 1989

approach for time discretization with the standard Galerkin finite element method for spatial approximation guarantees a proper matching of the two discretization processes, particularly in the treatment of the convective phenomena, which are dominant in many practical problems.

The content of the paper is organized as follows. In Section 2 the initial/boundary value problem for the unsteady flow of a viscous incompressible fluid is recalled and the proposed fractional-step solution procedure is briefly outlined. Section 3 deals with the numerical treatment of the convection phase in the Navier–Stokes equations. Section 4 describes the viscous diffusion phase, whereas Section 5 is devoted to the pressure/incompressibility phase. In Section 6 some features related to the finite element discretization are pointed out. Finally, Section 7 contains some numerical illustrations of the performance of the proposed fractional-step method.

2. GOVERNING EQUATIONS AND SOLUTION PROCEDURE

Let Ω be a bounded domain of $\mathbb{R}^d$, $d=2$ or 3, with a piecewise smooth boundary Γ. The motion of a viscous incompressible fluid is governed by the Navier–Stokes equations

$$\frac{\partial \mathbf{u}}{\partial t} + (\mathbf{u}\cdot\nabla)\mathbf{u} = \nabla\cdot\boldsymbol{\sigma}, \tag{1}$$

$$\nabla\cdot\mathbf{u} = 0, \tag{2}$$

where $\mathbf{u} = \mathbf{u}(\mathbf{x}, t)$ is the velocity and $\boldsymbol{\sigma} = \boldsymbol{\sigma}(\mathbf{u})$ is the total stress (per unit density of the fluid). We shall consider the case of a Newtonian fluid whose constitutive equation is given by

$$\boldsymbol{\sigma}(\mathbf{u}) = -p\mathbf{I} + 2\nu\mathbf{D}(\mathbf{u}). \tag{3}$$

Here $p = p(\mathbf{x}, t)$ is the pressure (per unit density), ν is the coefficient of kinematic viscosity, $\mathbf{I}$ is the unit tensor and $\mathbf{D}(\mathbf{u})$ is the deformation rate tensor defined by

$$\mathbf{D}(\mathbf{u}) = \tfrac{1}{2}[\nabla\mathbf{u} + (\nabla\mathbf{u})^{\mathrm{T}}]. \tag{4}$$

The boundary conditions considered here are

$$\mathbf{u}|_{\Gamma_1} = \mathbf{b}, \tag{5}$$

$$\mathbf{n}\cdot\boldsymbol{\sigma}(\mathbf{u})|_{\Gamma_2} = \mathbf{c} + \mathbf{d}, \tag{6}$$

where Γ_1 and Γ_2 are two disjoint non-overlapping subsets of the boundary Γ, $\mathbf{b}$ represents the velocity vector prescribed on Γ_1, $\mathbf{c}$ and $\mathbf{d}$ designate the pressure and the viscous part respectively of the traction vector prescribed on Γ_2, and $\mathbf{n}$ is the outward unit vector normal to Γ. If $\Gamma_1 = \Gamma$ and $\Gamma_2 = \varnothing$, the prescribed velocity $\mathbf{b}$ must satisfy the consistency condition

$$\oint_\Gamma \mathbf{n}\cdot\mathbf{b}\,\mathrm{d}\Gamma = 0. \tag{7}$$

In this case the pressure field p is determined up to an arbitrary additive constant value.

The initial condition consists of specifying the velocity field at the initial time $t = 0$, namely

$$\mathbf{u}(\mathbf{x}, 0) = \mathbf{u}_0(\mathbf{x}) \quad \text{with} \quad \nabla\cdot\mathbf{u}_0 = 0. \tag{8}$$

The calculation of transient solutions to the incompressible Navier–Stokes equations presents the following difficulties.

1. The non-linearity of the convective term makes an explicit treatment computationally

attractive, but it is not easy to assure a high-order accuracy in time using standard explicit methods.

2. The 'mixed' hyperbolic–parabolic character of the momentum equation can give rise to singular behaviour in the solution, particularly in regions where convection dominates over diffusion.
3. The elliptic character of the incompressibility condition requires an implicit treatment for the determination of the pressure.

In an attempt to overcome the above difficulties, a fractional-step approach for the time integration is adopted here, which permits the isolation of the effects of the various spatial operators. Accordingly, the proposed algorithm is divided into the following three phases: convection, viscous diffusion and incompressibility.

3. CONVECTION PHASE

In the convection phase, only the non-linear term in the momentum equation (1) is retained. The equation to be solved reduces therefore to the following hyperbolic vector equation:

$$\frac{\partial \mathbf{u}}{\partial t} + (\mathbf{u} \cdot \nabla)\mathbf{u} = 0. \tag{9}$$

A second-order Taylor–Galerkin method is used to obtain a discrete approximation of (9). The equation is first discretized in time by considering a Taylor series expansion in the (possibly variable) time step $\Delta t = t^{n+1} - t^n$ up to the second order:

$$\mathbf{u}^{n+1} = \mathbf{u}^n + \Delta t\, \mathbf{u}_t^n + \tfrac{1}{2}(\Delta t)^2 \mathbf{u}_{tt}^n + O[(\Delta t)^3]. \tag{10}$$

The first-order and second-order time derivatives in (10) are then expressed from the governing equation (9) in the form

$$\mathbf{u}_t = -(\mathbf{u} \cdot \nabla)\mathbf{u}, \tag{11}$$

$$\mathbf{u}_{tt} = -(\mathbf{u}_t \cdot \nabla)\mathbf{u} - (\mathbf{u} \cdot \nabla)\mathbf{u}_t = \{[(\mathbf{u} \cdot \nabla)\mathbf{u}] \cdot \nabla\}\mathbf{u} + (\mathbf{u} \cdot \nabla)[(\mathbf{u} \cdot \nabla)\mathbf{u}]. \tag{12}$$

The intermediate velocity field $\mathbf{u}^*$ resulting from the convection phase is then determined from $\mathbf{u}^n$ by means of equation (10) in which the time derivatives are replaced with the above expressions and $\mathbf{u}^{n+1} = \mathbf{u}^*$. This yields

$$\frac{\mathbf{u}^* - \mathbf{u}^n}{\Delta t} = -(\mathbf{u}^n \cdot \nabla)\mathbf{u}^n + \tfrac{1}{2}\Delta t\{[(\mathbf{u}^n \cdot \nabla)\mathbf{u}^n] \cdot \nabla\}\mathbf{u}^n + \tfrac{1}{2}\Delta t(\mathbf{u}^n \cdot \nabla)[(\mathbf{u}^n \cdot \nabla)\mathbf{u}^n]. \tag{13}$$

Equation (13) represents a time discretization of the Lax–Wendroff type for the vectorial convection equation written in non-conservative form. The scheme is second-order accurate in time. In this respect it is important to note that the second-order terms are not to be interpreted as a numerical diffusion or viscosity inherent to the scheme. Instead, these terms are an element of the improved difference approximation to the time derivative with respect to that associated with the explicit Euler algorithm.

A weak form of equation (13) is obtained by taking the scalar product with weighting functions $\mathbf{w} = \mathbf{w}(\mathbf{x})$ belonging to a suitable space of vector-valued functions and then integrating by parts the terms including second-order spatial derivatives. Let $(H^1(\Omega))^d$ denote the standard Sobolev space of vector functions defined on $\Omega \subset \mathbb{R}^d$ which are square integrable and have square integrable first-order derivatives. Standard vectorial calculations lead to the following weak formulation of the time-discretized convection equation (13): find $\mathbf{u}^* \in (H^1(\Omega))^d$ such that

$$\langle \mathbf{w}, \mathbf{u}^* - \mathbf{u}^n \rangle/\Delta t = -\langle \mathbf{w}, (\mathbf{u}^n \cdot \nabla)\mathbf{u}^n \rangle - \tfrac{1}{2}\Delta t[\langle (\mathbf{u}^n \cdot \nabla)\mathbf{w}, (\mathbf{u}^n \cdot \nabla)\mathbf{u}^n \rangle - \langle (\mathbf{n} \cdot \mathbf{u}^n)\mathbf{w}, (\mathbf{u}^n \cdot \nabla)\mathbf{u}^n \rangle_\Gamma] + \tfrac{1}{2}\Delta t \langle [\mathbf{w} \times \nabla \times \mathbf{u}^n + (\mathbf{w} \cdot \nabla)\mathbf{u}^n - \mathbf{w}(\nabla \cdot \mathbf{u}^n)], (\mathbf{u}^n \cdot \nabla)\mathbf{u}^n \rangle, \quad \forall \mathbf{w} \in (H^1(\Omega))^d, \tag{14}$$

where $\langle , \rangle$ denotes the integration over the domain Ω and $\langle , \rangle_\Gamma$ over the boundary Γ. The boundary conditions to be imposed in the convection phase are discussed later.

For reasons of computational efficiency it can be convenient to express equation (14) in an equivalent form by writing the first two terms in the last scalar product into a single expression. The problem now reads: find $\mathbf{u}^* \in (H^1(\Omega))^d$ such that

$$\langle \mathbf{w}, \mathbf{u}^* - \mathbf{u}^n \rangle/\Delta t = -\langle \mathbf{w}, (\mathbf{u}^n \cdot \nabla)\mathbf{u}^n \rangle - \tfrac{1}{2}\Delta t[\langle (\mathbf{u}^n \cdot \nabla)\mathbf{w}, (\mathbf{u}^n \cdot \nabla)\mathbf{u}^n \rangle - \langle (\mathbf{n} \cdot \mathbf{u}^n)\mathbf{w}, (\mathbf{u}^n \cdot \nabla)\mathbf{u}^n \rangle_\Gamma] + \tfrac{1}{2}\Delta t \langle \mathbf{w}, \{[(\mathbf{u}^n \cdot \nabla)\mathbf{u}^n] \cdot \nabla\}\mathbf{u}^n \rangle - \tfrac{1}{2}\Delta t \langle \mathbf{w}(\nabla \cdot \mathbf{u}^n), (\mathbf{u}^n \cdot \nabla)\mathbf{u}^n \rangle, \quad \forall \mathbf{w} \in (H^1(\Omega))^d. \tag{15}$$

The second-order terms present in (14) or (15) admit a simple physical interpretation. The most important term is the first one, namely

$$-\tfrac{1}{2}\Delta t \langle (\mathbf{u}^n \cdot \nabla)\mathbf{w}, (\mathbf{u}^n \cdot \nabla)\mathbf{u}^n \rangle. \tag{16}$$

It is present even in the case of a linearized version of the convection equation (uniform convection velocity). This term is block diagonal: the Cartesian components of the velocity vector are uncoupled. Each block is associated with a symmetric operator when $\mathbf{u}$ and $\mathbf{w}$ are chosen to belong to the same space (Galerkin method). Furthermore, such an operator has a tensorial structure which enables it to act only in the direction of the convection velocity and not transversely. In other words, it has a streamline character which is directly provided by the Lax–Wendroff time discretization without the need for any specific assumption or the introduction of a special parameter.

The second term in (14), proportional to Δt and involving volume integration, is

$$\tfrac{1}{2}\Delta t \langle [\mathbf{w} \times \nabla \times \mathbf{u}^n + (\mathbf{w} \cdot \nabla)\mathbf{u}^n - \mathbf{w}(\nabla \cdot \mathbf{u}^n)], (\mathbf{u}^n \cdot \nabla)\mathbf{u}^n \rangle. \tag{17}$$

It vanishes in the case of a uniform convection field and represents a correction to the leading quantity

$$-\langle \mathbf{w} + \tfrac{1}{2}\Delta t(\mathbf{u}^n \cdot \nabla)\mathbf{w}, (\mathbf{u}^n \cdot \nabla)\mathbf{u}^n \rangle. \tag{18}$$

The correction will be important or negligible depending on the measure of the non-uniformity of the convection velocity field as indicated by the three vector derivatives $\nabla \times \mathbf{u}^n$ (vorticity), $(\mathbf{w} \cdot \nabla)\mathbf{u}^n$ (variation of $\mathbf{u}^n$ in the direction of $\mathbf{w}$) and $\nabla \cdot \mathbf{u}^n$ (dilatation). The last contribution would be zero in the case of an exactly solenoidal velocity field. However, since the incompressibility condition is satisfied, in the present formulation, elementwise rather than pointwise, this contribution will be retained for internal consistency even though it is expected to be very small.

To discuss the meaning of the surface term resulting from the integration by parts, namely

$$\tfrac{1}{2}\Delta t \langle (\mathbf{n} \cdot \mathbf{u}^n)\mathbf{w}, (\mathbf{u}^n \cdot \nabla)\mathbf{u}^n \rangle_\Gamma, \tag{19}$$

it is necessary to analyse the boundary conditions imposed in the convection phase. Since the problem associated with equation (9) is hyperbolic, boundary values on Γ_1 can be prescribed only where the convection velocity is directed into the domain. Denoting by $\Gamma_{1,\mathrm{in}}^{n+1}$ the portion of the boundary Γ_1 such that $\mathbf{n}\cdot\mathbf{b}^{n+1} < 0$, the boundary condition for the convection phase will be

$$\mathbf{u}^*|_{\Gamma_{1,\mathrm{in}}^{n+1}} = \mathbf{b}^{n+1}. \tag{20}$$

Correspondingly, the weighting function $\mathbf{w}$ will be chosen to satisfy the homogeneous boundary condition $\mathbf{w}|_{\Gamma_{1,\mathrm{in}}^{n+1}} = 0$ and the surface integration will be limited to the complementary portion of the boundary where the flow velocity is directed outwards from the computational domain. In this way, and by its very structure, the surface term is capable of taking into account the outflow of the momentum along the streamlines of the convection field and assures good absorbing properties at outflow boundaries in transient calculations, as has been clearly demonstrated in the case of a scalar equation.[2]

4. VISCOUS DIFFUSION PHASE

This phase considers the viscous terms in the Navier–Stokes equations. From equations (1) and (3) one has

$$\frac{\partial \mathbf{u}}{\partial t} = \nabla\cdot[2\nu\mathbf{D}(\mathbf{u})]. \tag{21}$$

A first-order explicit (Euler) time integration scheme is used here so that a new intermediate velocity $\mathbf{u}^{**}$ is determined from $\mathbf{u}^*$ by solving the equation

$$\frac{\mathbf{u}^{**} - \mathbf{u}^*}{\Delta t} = \nabla\cdot[2\nu\mathbf{D}(\mathbf{u}^*)]. \tag{22}$$

The associated weak formulation is obtained, after integration by parts, in the following form: find $\mathbf{u}^{**}\in(H^1(\Omega))^d$ such that

$$\langle \mathbf{w}, \mathbf{u}^{**} - \mathbf{u}^* \rangle/\Delta t = -2\langle \nu\mathbf{D}(\mathbf{w}), \mathbf{D}(\mathbf{u}^*)\rangle + \langle \mathbf{w}, \mathbf{d}^n\rangle_{\Gamma_2}, \quad \forall \mathbf{w}\in(H^1(\Omega))^d, \quad \mathbf{w}|_{\Gamma_1} = 0. \tag{23}$$

The boundary conditions to be imposed in this phase are the velocity boundary conditions (5) on Γ_1, which read

$$\mathbf{u}^{**}|_{\Gamma_1} = \mathbf{b}^{n+1}, \tag{24}$$

and the viscous part of the stress boundary conditions (6) on Γ_2. The latter appears as a natural boundary condition, as shown by the surface term in equation (23).

It should be noted that a second-order implicit integration scheme, such as the Crank–Nicolson algorithm,[4] could easily be introduced in this phase.

5. PRESSURE PHASE AND INCOMPRESSIBILITY

The intermediate velocity field resulting from the above phases contains the effects of convection and viscous diffusion but does not satisfy the incompressibility condition. In the last phase the final velocity field $\mathbf{u}^{n+1}$ is determined from the intermediate velocity $\mathbf{u}^{**}$ by adding the dynamical effect of the pressure p^{n+1} determined so as to make the incompressibility condition satisfied. From equations (1) and (3) the pressure phase reads

$$\frac{\partial \mathbf{u}}{\partial t} = -\nabla p, \tag{25}$$

$$\nabla\cdot\mathbf{u} = 0. \tag{26}$$

Using a first-order implicit Euler scheme for the time discretization of (25), the following system of coupled equations for $\mathbf{u}^{n+1}$ and p^{n+1} is obtained:

$$\frac{\mathbf{u}^{n+1}-\mathbf{u}^{**}}{\Delta t}=-\nabla p^{n+1}, \tag{27}$$

$$\nabla\cdot\mathbf{u}^{n+1}=0. \tag{28}$$

Actually, the objective is to decompose the intermediate field $\mathbf{u}^{**}$ into the sum of a vector field with zero divergence and another with zero curl. The divergence-free component is the end-of-step velocity vector $\mathbf{u}^{n+1}$ whereas the irrotational one is related to the gradient of the pressure field p^{n+1}. Such a decomposition is associated with the presence of an operator of orthogonal projection (projection method).[6]

The weak formulation of problem (27), (28) is obtained, after integration by parts, in the form:[7] find $\mathbf{u}^{n+1}\in(H^1(\Omega))^d$ and $p^{n+1}\in L^2(\Omega)$ such that

$$\langle \mathbf{w},\mathbf{u}^{n+1}-\mathbf{u}^{**}\rangle/\Delta t=\langle\nabla\cdot\mathbf{w},p^{n+1}\rangle+\langle\mathbf{w},\mathbf{c}^{n+1}\rangle_{\Gamma_2},\quad\forall\mathbf{w}\in(H^1(\Omega))^d,\quad \mathbf{n}\cdot\mathbf{w}|_{\Gamma_1}=0, \tag{29}$$

$$\langle q,\nabla\cdot\mathbf{u}^{n+1}\rangle=0,\quad\forall q\in L^2(\Omega), \tag{30}$$

where $L^2(\Omega)$ denotes the Hilbert space of square integrable scalar functions and q is the weighting function associated with the continuity equation.

As far as the velocity boundary conditions are concerned, only the normal component of the velocity is imposed in this phase:[7]

$$\mathbf{n}\cdot\mathbf{u}^{n+1}|_{\Gamma_1}=\mathbf{n}\cdot\mathbf{b}^{n+1}. \tag{31}$$

Finally, the pressure loads prescribed on the portion Γ_2 of the boundary are imposed as natural boundary conditions in the surface term present in equation (29).

It is important to note that the problem (29)–(31) is the primal–dual form of an elliptic boundary value problem for the pressure. It is well known that the boundary conditions associated with a Poisson problem for the pressure in the fractional-step projection method consist of specifying the value of the pressure gradient normal to the boundary but not along the tangential direction. As a consequence, the velocity conditions on Γ_1 are imposed only for the normal component and not for the tangential ones, the latter being satisfied here in a weak sense only. This approach completely avoids the spurious spatial oscillations of pressure, known as chequerboarding.[8] A detailed discussion of this important issue is provided in Reference 7, where numerical solutions of the standard driven cavity problem (steady and unsteady) are presented. The imposition of the boundary condition (31) only for the normal component of velocity in the incompressible phase has been shown to yield a pressure field free from spatial oscillations, using both uniform and non-uniform meshes.

As with any other procedure of the fractional-step type, the combination of the three computational phases just described introduces time-splitting errors, which are, however, not discussed in the present paper. We only remark that the first-order discretization for the pressure phase and the second-order treatment of the other two phases combine to give a satisfactory numerical accuracy when the temporal variation of the velocity field is caused mainly by advection and/or viscous diffusion effects.

6. FINITE ELEMENT DISCRETIZATION

The fully discrete form of equations (14), (20), (23)–(24) and (29)–(31) are subsequently obtained by means of the conventional Galerkin–Bubnov finite element method. The flexibility and accuracy of this method are well recognized. Four-noded isoparametric elements with bilinear shape functions for the velocity and elementwise constant approximation for the pressure are considered.

The convection phase, though being based on an explicit time integration algorithm, requires the inversion of the mass matrix. The importance of including the consistent mass matrix in transient convective transport problems was originally demonstrated by Gresho *et al.*[9] The solution of the associated system of linear equations can be performed very efficiently in regular domains with a Cartesian mesh of quadrilateral elements by means of the algorithm developed by Staniforth and Mitchell.[10,11] On the other hand, in the case of a general mesh the inversion of the mass matrix can be performed approximately by means of an iterative procedure of the Jacobi type.[4] By virtue of the symmetric and diagonally dominant character of the matrix, the procedure converges in a few iterations. Three iterations are employed here to preserve the high phase-speed accuracy of the spatial discretization considered. On the contrary, in the viscous diffusion phase an approximation in one iteration is employed, which corresponds to the standard diagonal lumped matrix obtained by the row-sum technique. Such an approximation is well justified in the context of explicit time integration of parabolic equations. The same approximation is also applied in the pressure phase and has been justified for different reasons.[7]

The system obtained from equations (29) and (30) represents a linear system of coupled equations for the final velocity and pressure. A symmetric system of linear equations for the pressure can be derived and solved via a direct method such as the Cholesky decomposition. Once the pressure has been obtained, the final velocity is then computed (see Reference 7 for details).

In the proposed method the time step Δt will be restricted by conditions of numerical stability. The condition to be considered in the convection phase has been discussed in detail for the two-dimensional case in Reference 2. In this connection it is worth mentioning that the time accuracy for the convection phase can be increased to the third order by applying the two-step procedure suggested by Selmin.[12] This amounts to solving in sequence two second-order schemes of the type discussed herein, but with appropriately modified coefficients. The resulting third-order scheme clearly requires twice the computational effort needed by its second-order counterpart, but has the advantage of a substantial enlargement of the domain of numerical stability in two and three space dimensions.[12]

The stability limits to be used in the viscous diffusion phase follow from the standard condition valid for a scalar diffusion equation in two dimensions.

7. NUMERICAL EXAMPLES

7.1. *Vortex shedding*

The evolution of twin vortices behind a flat plate has been calculated and compared with numerical[13] and experimental[14] results. The experiment has carried out in a water tank 0·40 m wide. A thin test plate of size $H = 0{\cdot}03$ m immersed in the water was impulsively started from rest at the velocity ($u_1 = U = 4{\cdot}95 \times 10^{-3}$ m s^{-1}). The outlet boundary is assumed to be traction-free. Along the other two boundaries the tangential tractions and the normal velocity components are assumed to be zero. A no-slip condition is prescribed at the plate surface. The initial condition is $\mathbf{u} = 0$ at $t = 0$. The fluid density is $\rho = 998{\cdot}0$ kg m^{-3} and the dynamic viscosity $\mu = 1{\cdot}008 \times 10^{-3}$ Pa s.

Since the geometry and the boundary conditions are symmetric, only the lower half of the tank has been modelled. A constant time step size $\Delta t = 25$ s has been chosen. The selected finite element mesh and the problem data are shown in Figure 1.

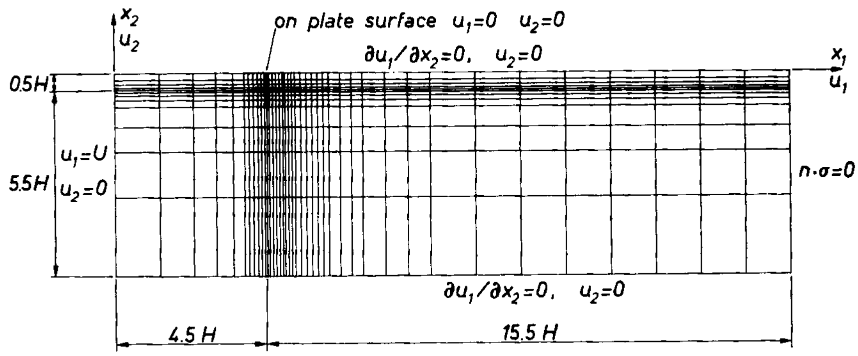

Figure 1. Vortex shedding; finite element mesh and boundary conditions

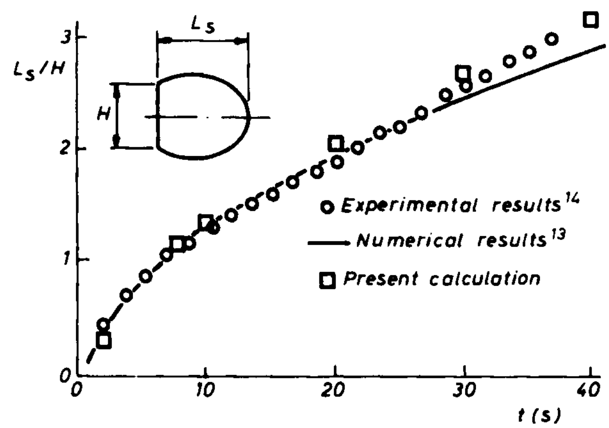

Figure 2. Vortex shedding; movement of the stagnation point (comparison with experimental and other numerical results)

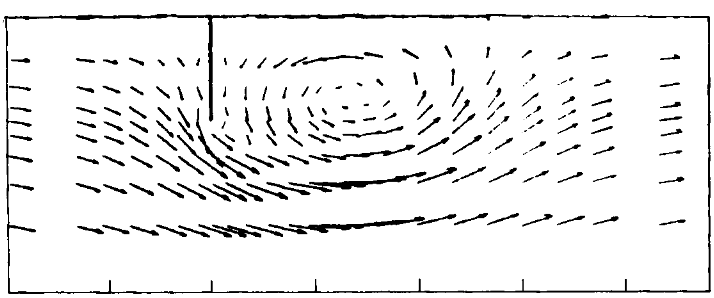

Figure 3. Vortex shedding; velocity vectors at $t = 8$ s

The calculated time history of the stagnation point position is reported in Figure 2 together with experimental and other numerical results. The calculated velocity field at the time $t = 8$ s is shown in Figure 3. The present results are in excellent agreement with those reported in the referenced works.[13,14]

7.2. *Plane jet simulation*

A plane jet problem is considered in which the flow domain is the right half-space $\{x|x_1 > 0, x_2 \in \mathbb{R}\}$. The viscosity is assumed to be $\nu = 5 \times 10^{-4}$ and the density $\rho = 1$ (non-dimensional variables are used). The fluid is at rest at $t = 0$ and the jet aperture is located on the line $x_1 - 0$ centred at $\mathbf{x} = (0, 0)$ and is 1/16 wide. The jet profile is parabolic with a maximum velocity equal to unity, the jet being horizontal at $x_1 = 0$. The corresponding Reynolds number is $Re = 125$. The computational domain defined by $]0, 1[\times] -\frac{1}{2}, +\frac{1}{2}[$ is discretized by a 32×32 uniform mesh of the four-noded elements. The time step is taken to be $\Delta t = 0{\cdot}01$. The flow pattern, particularly the vortex creation close to the jet aperture, is represented at different times in Figure 4 and is in

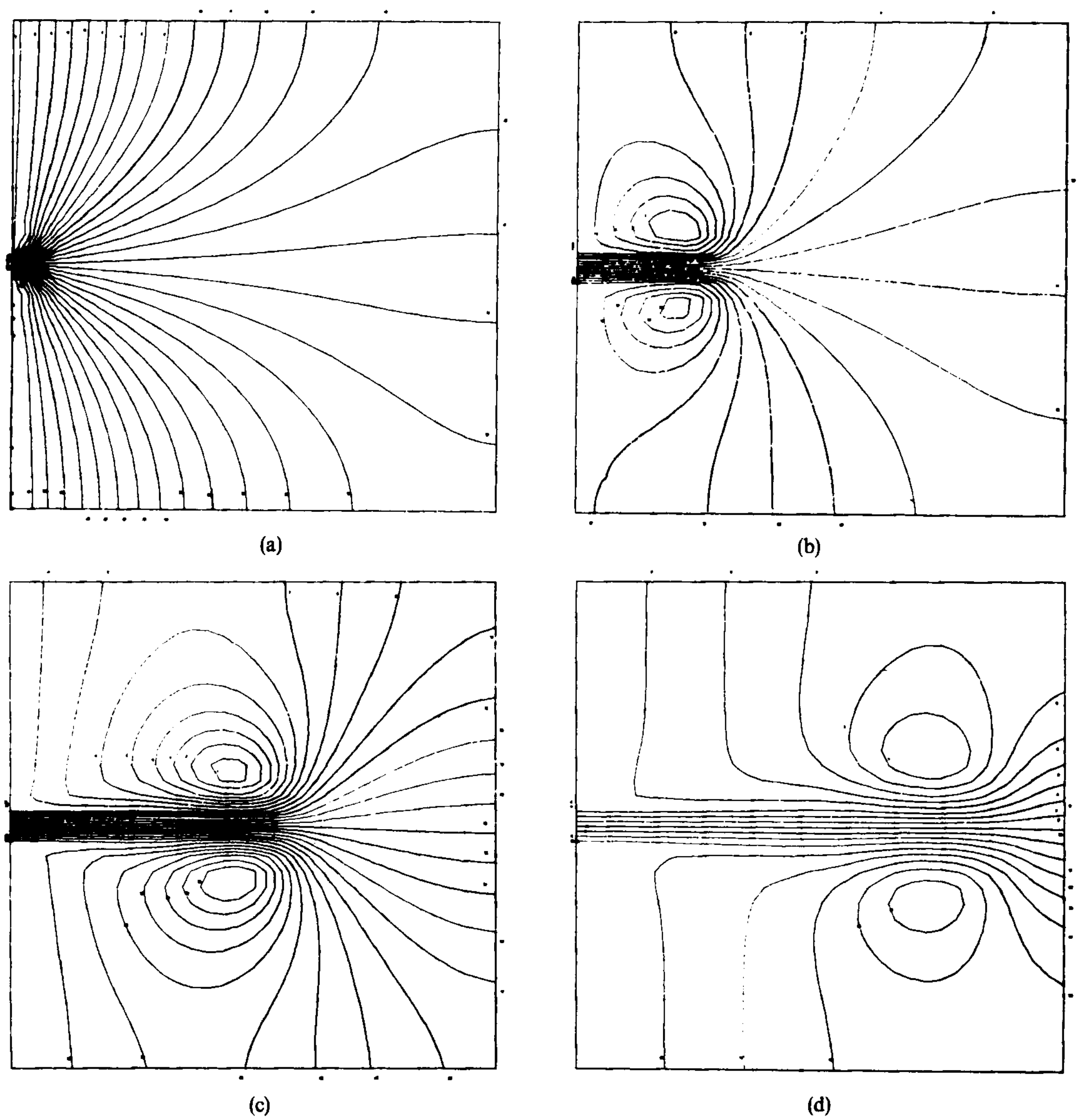

Figure 4. Plane jet ($Re = 125$); streamfunction distribution: (a) $t = 0{\cdot}1$ ($\Delta\psi = 10^{-3}$); (b) $t = 1{\cdot}2$ ($\Delta\psi = 2{\cdot}5 \times 10^{-4}$); (c) $t = 2{\cdot}5$ ($\Delta\psi = 2{\cdot}5 \times 10^{-3}$); (d) $t = 4{\cdot}0$ ($\Delta\psi = 5 \times 10^{-3}$)

good agreement with the results of Bristeau *et al.*[15] The corresponding pressure distributions are given in Figure 5.

7.3. *Flow over a square obstacle*

A sketch depicting the geometry of the flow domain, the discretization and the boundary conditions is given in Figure 6. At the inlet a constant uniform velocity is imposed, while at the outlet, traction-free conditions are considered. Along the other boundaries and along the

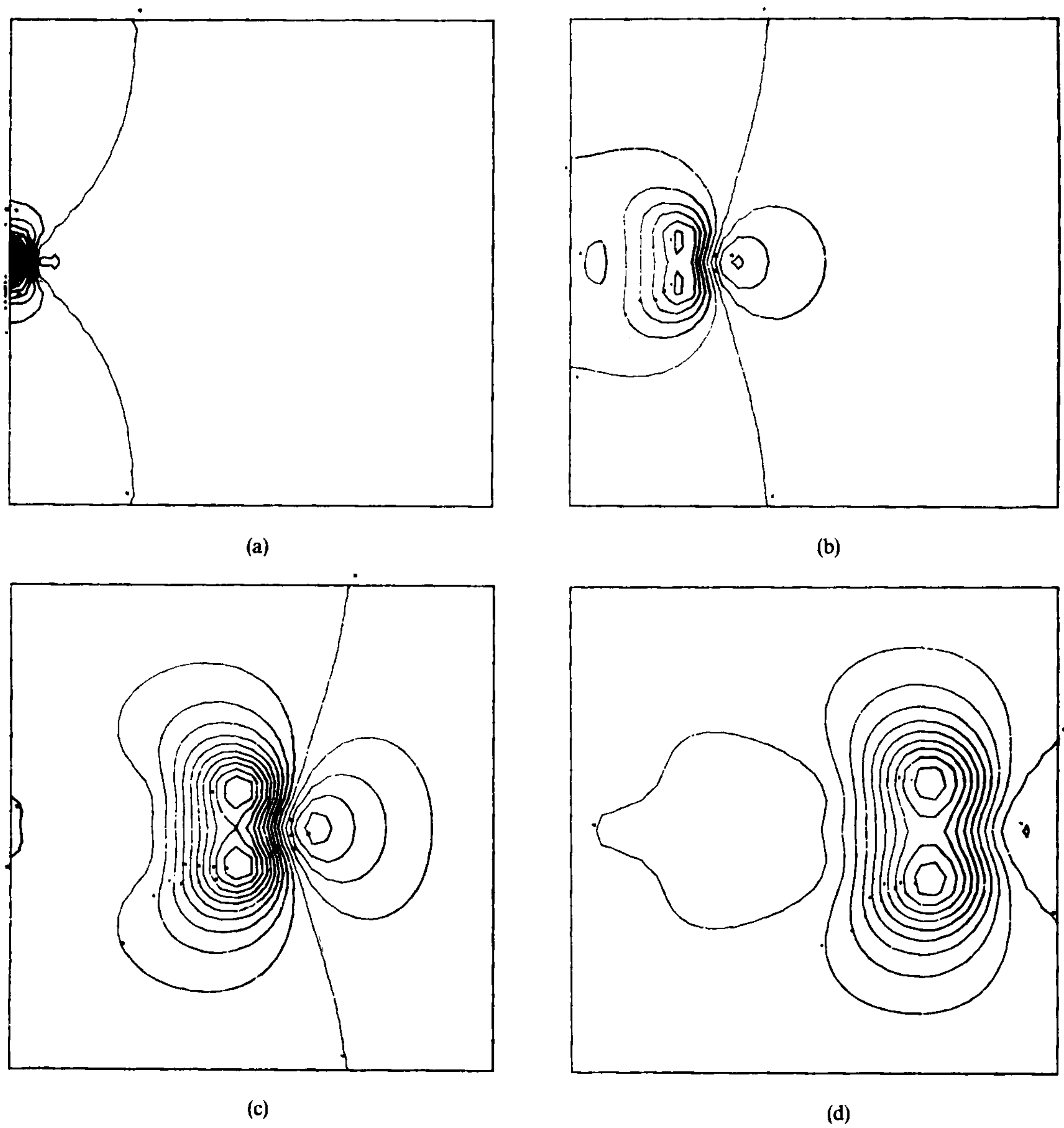

Figure 5. Plane jet ($Re = 125$); pressure contours: (a) $t = 0{\cdot}1$ ($\Delta p = 10^{-2}$); (b) $t = 1{\cdot}2$ ($\Delta p = 10^{-2}$); (c) $t = 2{\cdot}5$ ($\Delta p = 5 \times 10^{-3}$); (d) $t = 4{\cdot}0$ ($\Delta p = 5 \times 10^{-3}$)

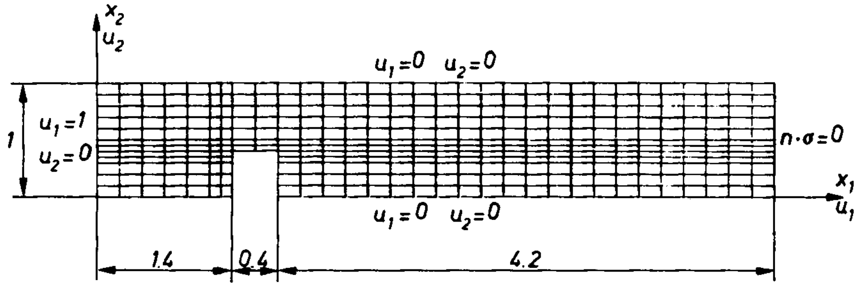

Figure 6. Flow over a square obstacle; geometry, finite element mesh and boundary conditions

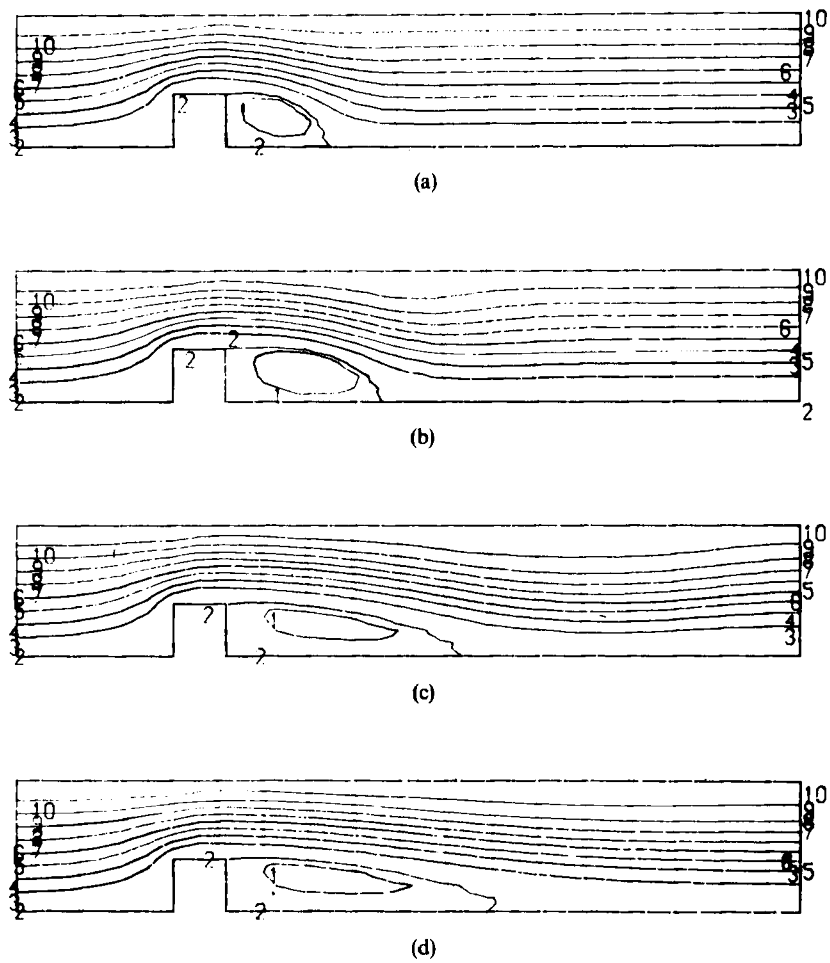

Figure 7. Flow over a square obstacle ($Re = 200$); streamfunction distribution: (a) $t = 1{\cdot}0$; (b) $t = 2{\cdot}0$; (c) $t = 5{\cdot}0$; (d) $t = 50{\cdot}0$ (ψ-values are 0·02, 0·0(−0·1)−0·8 for isolines 1–10)

obstacle, no-slip conditions are considered. The viscosity is taken to be $\nu = 5 \times 10^{-3}$ and the density $\rho = 1$ (non-dimensional variables are used), corresponding to $Re = 200$. The calculation has been performed up to the time $t = 50$, at which the flow has reached a steady state. The flow evolution in time is represented in Figure 7 by the streamline distributions at $t = 1{\cdot}0$, 2·0 5·0 and

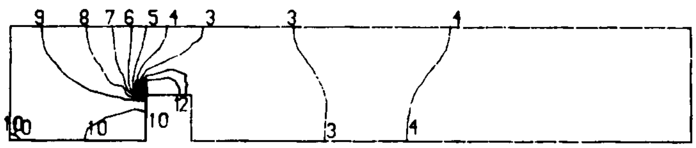

Figure 8. Flow over a square obstacle ($Re = 200$); pressure contours at $t = 50{\cdot}0$ (p-values are $-0{\cdot}7(0{\cdot}2)1{\cdot}1$ for isobars 1–10)

50·0, while the pressure pattern at the final time is shown in Figure 8. The maximum value of the streamfunction in the recirculation region at the steady state is found to be $\psi_{max} = 0{\cdot}034$, which compares well with the value $\psi_{max} = 0{\cdot}038$ obtained on the same mesh but using biquadratic approximations.[16]

8. CONCLUSIONS

A transient finite element methodology has been presented for solving incompressible viscous flow problems. The salient feature of the proposed method is a fractional-step approach to the numerical time integration of the unsteady Navier–Stokes equations in which the convective, viscous and pressure terms are treated in three distinct phases. A second-order accurate explicit Taylor–Galerkin method is introduced in the convection phase. This is followed by a first-order explicit treatment of the viscous diffusion phase. Finally, a first-order implicit scheme is used in the pressure phase, the pressure being determined so that the incompressibility condition remains satisfied.

The advantages of the proposed method are its extremely simple algorithmic structure, the ease of implementation of new solution algorithms for the various phases as they eventually become available, and its straightforward extension to deal with three-dimensional simulations and turbulence modelling. The numerical examples discussed in the paper indicate that, in addition to its simplicity, the proposed method is capable of producing accurate results.

REFERENCES

1. J. Donea, 'A Taylor–Galerkin method for convective transport problems', *Int. j. numer. methods eng.*, **20**, 101–119 (1984).
2. J. Donea, L. Quartapelle and V. Selmin, 'An analysis of time-discretization in the finite element solution of hyperbolic problems', *J. Comput. Phys.*, **70**, 463–499 (1987).
3. J. Donea, V. Selmin and L. Quartapelle, 'Recent developments of the Taylor–Galerkin method for the numerical solution of hyperbolic problems', in K. W. Morton and M. J. Baines (eds), *Numerical Methods for Fluid Dynamics III*, Clarendon Press, 1989, pp. 171–185.
4. J. Donea, S. Giuliani, H. Laval and L. Quartapelle, 'Time-accurate solution of advection–diffusion problems', *Comput. Methods Appl. Mech. Eng.*, **45**, 123–146 (1984).
5. W. Koschel, M. Lotzerich and A. Vornberger, 'Explicit method for solving Navier–Stokes equations using a finite element formulation', in E. H. Hirschel (ed.), *Notes in Fluid Mechanics, Vol. 14*, Vieweg, 1986, pp. 148–160.
6. A. J. Chorin, 'Numerical solution to the Navier–Stokes equations', *Math. Comput.*, **22**, 745–762 (1968).
7. J. Donea, S. Giuliani, H. Laval and L. Quartapelle, 'Finite element solution of the unsteady Navier–Stokes equations by a fractional step method', *Comput. Methods Appl. Mech. Eng.*, **30**, 53–73 (1982).
8. R. L. Sani, P. M. Gresho, R. L. Lee, D. F. Griffiths and M. Engelman, 'The cause and cure (?) of the spurious pressures generated by certain FEM solutions of the incompressible Navier–Stokes equations: Parts 1 and 2', *Int. j. numer. methods fluids*, **1**, 17–44, 171–204 (1981).
9. P. M. Gresho, R. L. Lee and R. Sani, 'Advection-dominated flows with emphasis on the consequences of mass lumping', in *Finite Elements in Fluids, Vol. 3*, Wiley, 1978, pp. 325–342.
10. A. N. Staniforth and H. L. Mitchell, 'A variable-resolution finite-element technique for regional forecasting with the primitive equations', *Mon. Weather Rev.*, **106**, 439–447 (1978).

11. A. N. Staniforth, 'Review: Formulating efficient finite-element codes for flows in regular domains', *Int. j. numer. methods fluids*, **7**, 1–16 (1987).
12. V. Selmin, 'Third-order finite element schemes for the solution of hyperbolic problems', *INRIA Report 707*, 1987.
13. Y. Yoshida and T. Nomura, 'A transient solution method for the finite element incompressible Navier–Stokes equations', *Int. j. numer. methods fluids*, **5**, 873–890 (1985).
14. S. Taneda and H. Honji, 'Unsteady flow past a flat plate normal to the direction of motion', *J. Phys. Soc. Japan*, **30**, 262–273 (1971).
15. M. O. Bristeau, R. Glowinski and J. Periaux, 'Numerical methods for the Navier–Stokes equations. Applications to the simulation of compressible and incompressible viscous flows', *Comput. Phys. Rep.*, **6**, 73–187 (1987).
16. J. M. Leone and P. M. Gresho, 'Finite element simulations of steady, two-dimensional, viscous incompressible flow over a step', *J. Comput. Phys.*, **41**, 167–191 (1981).